Kuwait J.Sci., Vol.50, No.(3B),July.2023,pp(1-10)

The effect of mixing nanoparticles on the suspension physical stability

Fairooz F. Kareem*, Asrar A. Saeed, Mahasin F. Al-Kadhemy, Farah J. Kadhum

Dept. of Physics, Mustansiriyah University, College of Science, Baghdad, Iraq

Corresponding author: cenderlla78@yahoo.com

Abstract

Energy transfer in a hybrid mixture of Rhodamine 6G (Rh6G) dye laser as a donor and nanoparticles (NPs) as an acceptor were studied. The absorption spectra of 1×10^{-5} M of Rh6G in distilled water showed an increase in peak intensity upon addition of NPs. Notably, the spectra were improved upon addition of Aluminum Oxide (Al_2O_3) NPs. The addition of NPs quenches the fluorescence spectra of Rh6G due to Förster resonance energy transfer (FRET). The efficiency of this energy transfer increases with an increasing concentration of NPs, and a best value of efficiency of energy transfer was found for the Rh6G/Magnesium Oxide (MgO) NP system. A similarly strong relationship was also found for for the Rh6G/Al_2O_3 NP system.

Keywords: Absorption spectrum; Al_2O_3 NPs and MgO NPs; energy transfer efficiency; fluorescence spectrum; Rh6G dye laser.

1. Introduction

The Rhodamine 6G (Rh6G) molecule is an environmentally benign and widely used organic colourant/dye. It has a high fluorescence quantum yield and is water soluble, despite its innate hydrophobic attraction (Lin, Katla & Perez-Mercader, 2021). Rh6G is used in a wide variety of applications because of these characteristics, including in the imaging of cellular or polymeric samples and as an active medium in dye laser applications. It also sees wide use in petroleum dyeing, paper printing, forensic technology, colour photography, cosmetic product additives, laser technology, optical conversion, solar cells, diodes, signal amplification in optics, optical communications, optoelectronics (Al-Kadhemy, Abbas & Abdalmuhdi, 2020). Ionic dyes self-associate to varying degrees in solution, depending on a variety of conditions such as dye concentration, dye structure, temperature, pH, and solvent, among others, resulting in a deviation from Beer's law (Terdale & Tantray, 2017). With respect to functional physical properties, the solvent in which the dye is dissolved plays an important role. Stokes' shifts, fluorescence quantum yields, fluorescence durations, and both radiative and non-radiative rate constants all adhere to a more-or-less linear relationship with the solvent polarity in moderate to high polarity solvents (Barik & Nath, 2003).

There is an ever-increasing application of metal oxide NPs in numerous disciplines such as cosmetic production, electronics, material sciences, catalysis, environmental sciences, energy, and biomedicine (Moorthy *et al.*, 2015). Microelectronics, diagnostics, and biomolecular detection are all potential uses for magnesium oxide (MgO) NPs (Ali *et al.*, 2020). In the field of catalysis, the unique structure of aluminium oxide (Al_2O_3) is employed as the foundation for active phases that are subsequently coated with other materials (Chavali & Nikolova, 2019). The

unit cell of Al_2O_3 belongs to the rhombohedral system of crystal structures, Al_2O_3 exhibits a range of polymorphic forms, including γ-, θ-, κ -, and α -, whereby the α - phase has been determined to be stable, whilst the other phases have been deemed metastable (Abdullah, 2021). When dyes or dye-marked receptors are in close proximity to or associated with NPs, energy transfer or electron transfer can quench their fluorescence (Yun, Javier and Strouse, 2005). The non-radiative process of Förster resonance energy transfer (FRET) involves an electronically-excited donor transmitting its excitation energy to an acceptor, resulting in a drop in fluorescence intensity and the donor's excited state lifetime (Mokashi, Patil & G.B.Kolekar, 2012). For this process to be efficient, the energy gap between the ground state and the excited energy level of the donor and acceptor must be suitably matched. This means that the fluorescence emission spectra of the donor must overlap with the absorption spectrum of the acceptor and vice versa. An optimal distance for the transmission of excitation energy from the donor to the acceptor must also be maintained (Zhang, Wang & Liang, 2015). Saeed et al. demonstrated that changing the mass of Ag NPs present led to enhanced absorption in the absorption spectra of Rh6G dye solution, but this same mass change actually quenched the fluorescence spectra (Saeed, Al-Kadhemy & Al-Arab, 2018). Kareem et al. determined the optimum concentration of Rh6G in (1×10^{-5}) aqueous solution for absorption and the fluorescence spectra with respect to the Beer-Lambert law to be 525 and 554 nm, respectively (Kareem, Saeed & Kadhemy, 2021).

The aim of this study is to characterize the energy transfer of Rh6G dye (as a donor) and NPs (as acceptors) in the liquid phase with distilled water acting as a solvent. Further, we explore the effect of the addition of metal oxide NPs to Rh6G dye.

The aim of this study is to characterize the energy transfer of Rh6G dye (as a donor) and NPs (as acceptors) in the liquid phase with distilled water acting as a solvent. Further, we explore the effect of the addition of metal oxide NPs to Rh6G dye.

2. Theoretical Background

After transmitting its excitation energy to an acceptor molecule, A, an excited donor molecule D* relaxes and emits a photon. The dipole-dipole coupling interaction between the donor and acceptor causes non-radiative energy transfer, which does not warrant photon emission or re-absorption. This process, described by Thompson and Messina (2019) can be explained as follows:

$$D^{*}+A\rightarrow D + A^{*} \quad (1)$$

Energy transfer leads to a reduction in or the quenching of donor fluorescence and thus a decrease of excited state lifetime (Lewkowics & Lakowicz, 2006).

The energy-transferring efficiency E, originally determined by Wahba, El-Enany and Belal (2015), can be expressed as:

$$\boldsymbol{E = 1 - \frac{F_i}{F_{iO}}} \quad (2)$$

Where F_{iO} and F_i are the fluorescence intensity of the donor dye in the absence and presence of and acceptor molecule, respectively.

The Stern–Volmer relationship, as given in eq. (3), is used to discover the kinetics of a photophysical intermolecular deactivation process (quenching). In general, this process can be represented by a simple equation as determined by Yang, Xi and Yang (2005):

$$\frac{F_{iO}}{F_i} = 1 + K[Q] \quad (3)$$

Where *K* is the Stern-Volmer quenching constant and [Q] is the quencher concentration. Thus, a plot of F_{iO}/F_i versus [Q] should yield a straight line with a slope equal to K.

3. Experimental

Rh6G ($C_{28}H_{31}N_2O_3Cl$), with a molecular weight of 479.02 g·mol^{-1} was obtained from Sigma-Aldrich. Rh6G was dissolved in distilled water (di-H_2O), whose polarity was considered to be 10.2 D (Lide, 2010). Magnesium oxide (MgO) with an average particle diameter of 40 nm and purity of 99.9% was obyained from Intelligent Materials Pvt. Ltd. Aluminium oxide (Al_2O_3), with an average particle diameter of 20-30 nm and a purity of 99.9% was obtained from China. Photographs of the chemicals in powder form used in this study are shown in Figure 1 (A-C).

Rhodamine 6G Powder Magnesium Oxide NPs Aluminum Oxide NPs

Fig. 1. Chemicals (in powder form) used in the work

Dissolving the required quantity of Rh6G dye, weighted using a Mettler balance sensitive to 0.1 mg, in each solvent yielded a solution with a primary concentration of 1×10^{-2} M. The amount of dye, m, in grams (g) was calculated using equation (4), given by Al-Kadhemy, Hussein and Ali A. Dawood Al-Zuky (2012):

$$m = \frac{M_W VC}{1000} \quad (4)$$

Where Mw denotes dye molecular weight (g/mole), V denotes solvent volume (ml), and C denotes dye concentration (M). The dye was then diluted to obtain concentrations in the range of 1×10^{-2} - 1×10^{-6} M according to eq. (5) given by Ali and Zainab F. Mahdi (2012):

$$C_1 V_1 = C_2 V_2 \quad (5)$$

Where C_1 represents the high concentration, V_1 represents the volume before dilution, C_2 represents the low concentration, and V_2 represents the total volume after dilution. It was observed that the prepared solutions have a good homogeneity. Figure 2 shows the solutions of Rh6G in the concentration range of 1×10^{-2} - 1×10^{-6} M

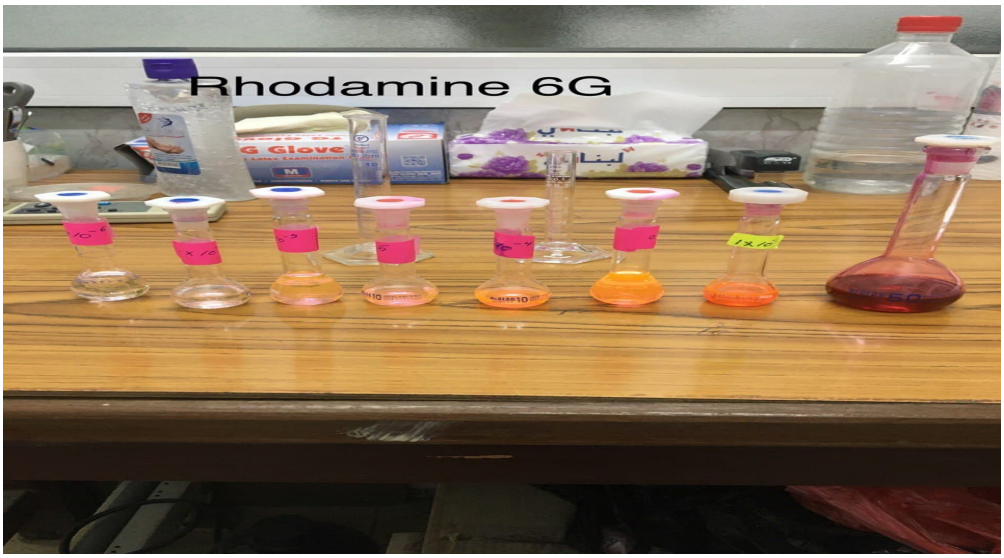

Fig. 2. Various concentrations of Rh6G in distilled water

The masses of MgO and Al_2O_3 used in this study were 2.0×10^{-3} and 4.0×10^{-3} g, respectively and were investigated by addition to dye solution. All the samples were prepared by mixing with the use of a hot plate with a magnetic stirrer for approximately one hour until the NPs were dispersed homogeneously throughout the Rh6G solution. All the samples were kept in the dark so as to avoid possible photo-bleaching or fading of the dye. The samples were used immediately after preparation.

A UV-Visible spectrophotometer (T70/T80) was used to record the absorption spectra of all samples, while a Spectrofluorometer was used to record the fluorescence spectra (SHIMATDZU RF-5301pc).

4. Results and Discussion

Figures 3 and 4 show the absorption and fluorescence spectra for Rh6G in distilled water. The maximum absorption wavelength (λ_{abs}) was found to be 525 nm, in good agreement with Kruszewski and Cyrankiewicz (2013), with a shoulder peak at 495 nm. The maximum fluorescence wavelength (λ_{fluo}) was 555 nm, which is in good agreement with Chen et al. (2008).

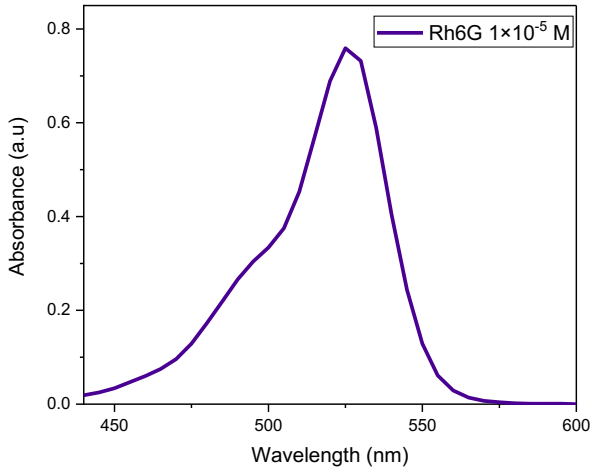

Fig. 3. Absorption spectrum of Rh6G in distilled water

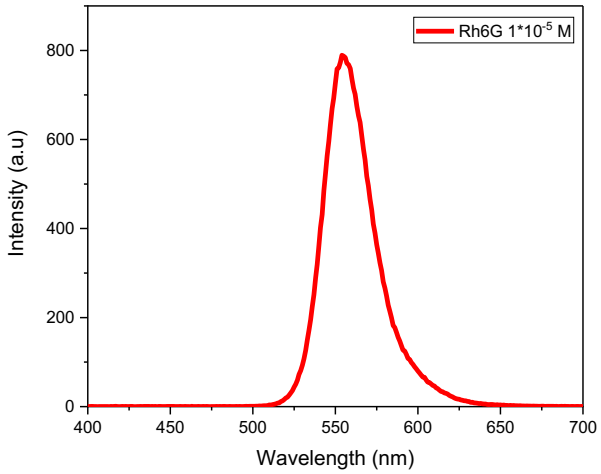

Fig. 4. Fluorescence spectrum of Rh6G in distilled water

Addition of MgO or Al_2O_3 NPs resulted in the Rh6G-NP solution having an enhanced absorption spectrum. At all NP concentrations, the maximum absorption wavelength was found to be consistent at 525 nm. The the addition of NPs caused an increase in the absorbance spectrum of Rh6G; when 4.0×10^{-3} g of Al_2O_3 NPs adding, absorbance rose to 1.92, while when 0.004g of MgO NPs were added, absorbance rose to 1.89, as demonstrated in in Table 1 and Figure 4. As a result of the addition of NPs, the photophysical characteristics of Rh6G dye were improved. The absorbance increases to 1.68 when 2.0×10^{-3} g of MgO NPs and 2.0×10^{-3} g of Al_2O_3 NPs in combination. It can be concluded that Al_2O_3 NPs has a large effect, but widens the spectrum's absorption peak. The absorption spectra increased with an increase in NP particle size, which can be explained as with Al being a metal, it may generate electrons and transform to a cation. Al_2O_3 NPs may also absorb water, making them useful as a drying agent. Due to its great stability, it is also considered an oxidizing agent (Stojanovic, Bukvic and Epler, 2018). The full width at half maximum (FWHM) of the absorption spectra increase with an increasing NP concentration in the case of Al_2O_3, whereas it decreases in the cases of MgO and mixed MgO-Al_2O_3 nanoparticle addition.

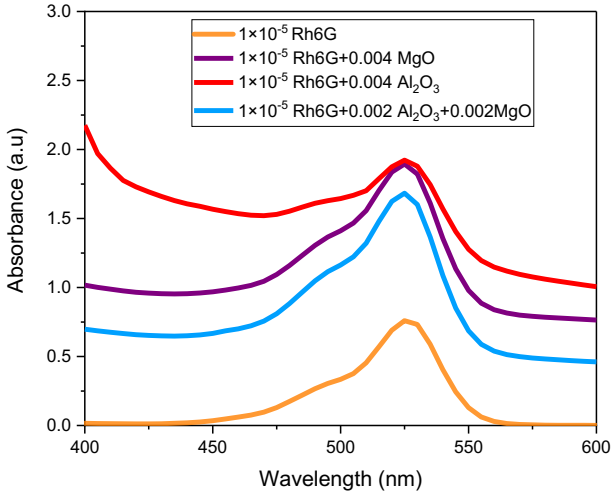

Fig. 5. Absorption spectra of Rh6G laser dye with 2.0×10^{-3} and 4.0×10^{-3} g of MgO and Al_2O_3 NPs.

Figure 6 and Table 1 show the fluorescence spectra of Rh6G with 2.0×10^{-3} and 4.0×10^{-3} g of MgO and Al_2O_3 NPs in all concentrations, where the highest fluorescence wavelength of 555 nm is seen. In Rh6G aqueous solution, the wavelength is 554 nm. A decrease in the intensity upon addition of MgO, Al_2O_3, or mixed MgO-Al_2O_3 NPs to Rh6G aqueous solution is seen. It should be noted that adding NPs led to decrease in the fluorescence intensity with an increase masse of NPs, while the maximum fluorescence peak remains constant. Non-radiative energy transfer between laser dyes and NPs is most likely to be the cause for the emission quenching. (Błaszkiewicz, Kotkowiak & Dudkowiak, 2017). The FWHM for fluorescence spectra increased with the addition of Al_2O_3 NPs, whilst it decreased with the addition of MgO or mixed MgO-Al_2O_3 NPs.

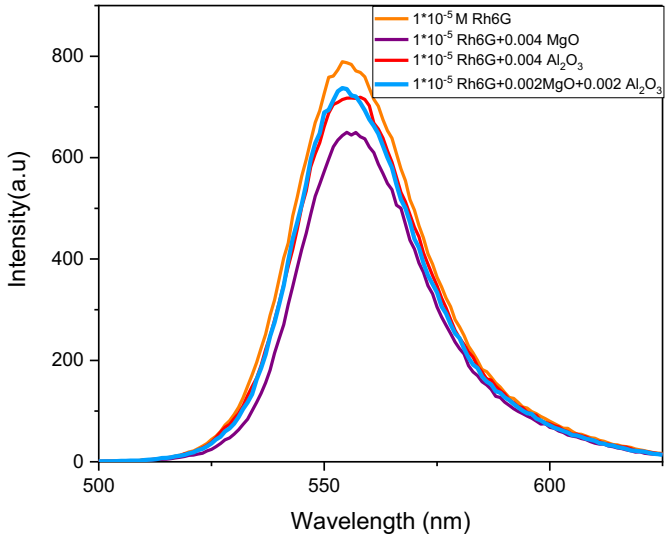

Fig. 6. Fluorescence spectra of Rh6G laser dye with 2.0×10^{-3} and 4.0×10^{-3} g of MgO and Al_2O_3 NPs.

Table 1. Spectral information for Rh6G aqueous solution with addition of NPs

Rh6G 1×10^{-5} M	Amount of MgO NPs (g)	Amount of Al_2O_3 NPs (g)	$\lambda_{abs\ max}$ (nm)	I_{abs}	FWHM (nm)	$\lambda_{fluo\ max}$ (nm)	I_{Fluo}	FWHM (nm)
	0	0	525	0.75	35	554	789.16	32.96
	0.004	0	525	1.89	58.30	555	649.9	31.83
	0	0.004	525	1.92	83.65	555	717.44	33.12
	0.002	0.002	525	1.68	56.31	555	735.34	31.55

Figure 6 shows the Stern-Volmer plot of 1×10^{-5} M Rh6G aqueous solution with the addition of 2.0×10^{-3} and 4.0×10^{-3} g of MgO NPs. The R^2 metric of goodness-of-fit is almost equal to 1, which means there is a strong relationship between the two parameters (line and point). Furthermore, the Stern-Volmer relationship calculated from equation (3) is found to be 54.87 M^{-1}. All of the samples studied had linear Stern-Volmer dependence, implying a single quenching process (Błaszkiewicz, Kotkowiak & Dudkowiak, 2017).

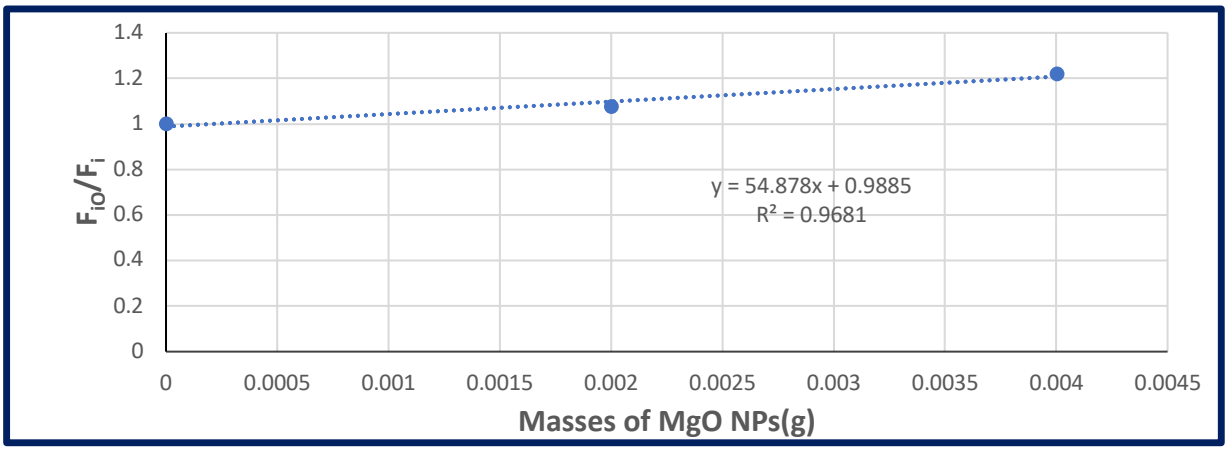

Fig. 7. Stern-Volmer plot of Rh6G with MgO NPs

Additionally, Table 2 show the efficiency of energy transfer of Rh6G with MgO NPs. As the amount ofcMgO NPs present increases, an increase the energy transfer efficiency is also seen, which can be described by the efficiency of Stern-Volmer equation (2). The curve of Rh6G with MgO NPs can also be regarded as a straight line in low concentration where the ratio here is <10 (Yang, Xi & Yang, 2005).

Table 2. Energy-transfer efficiencies for Rh6G dye with MgO NPs

	Amount of MgO NPs (g)	F_{iO}	F_i	E
Rh6G 1×10^{-5} M	0	789.16	789.16	0
	0.002	789.16	735.34	0.07
	0.004	789.16	649.9	0.18

Figure 8 and Table 3 display the Stern-Volmer relationship and energy transfer of 1×10^{-5} M Rh6G dye solution in distilled water with 2.0×10^{-3} and 4.0×10^{-3} g masses of Al_2O_3 NPs. Again, the R^2 value is very close to 1 indicating a strong linear dependence. The Stern-Volmer quenching constant, K, is 27.778 M^{-1} when it calculated from the eq. (2). Table 3 demonstrates that increasing the amount of Al_2O_3 NPs leads to an increase in the efficiency of energy transfer.

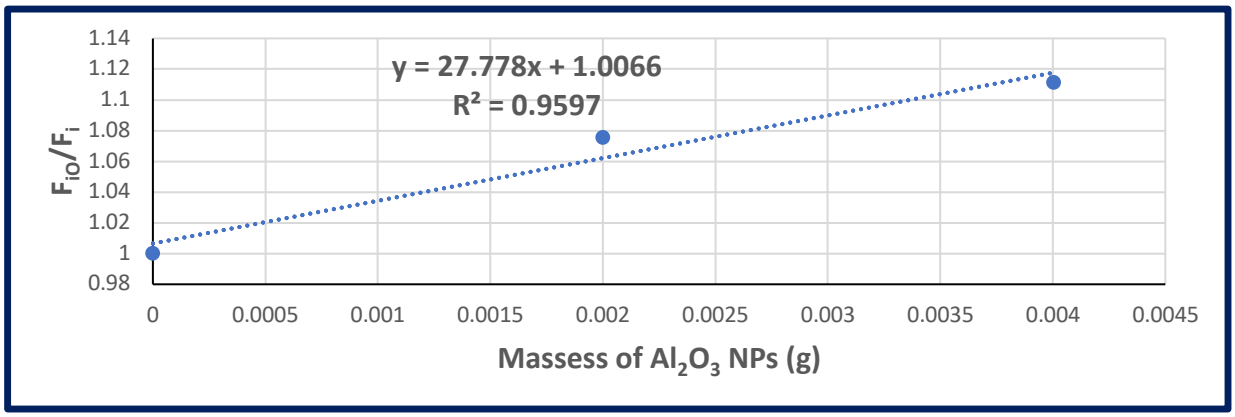

Fig. 8. Stern-Volmer plot of Rh6G with Al_2O_3 NPs

Table 3. Energy-transfer efficiencies for Rh6G dye with Al_2O_3 NPs

Rh6G 1×10^{-5} M	Amount of Al_2O_3 NPs(g)	F_{iO}	F_i	E
	0	789.16	789.16	0
	0.002	789.16	735.34	0.07
	0.004	789.16	717.44	0.1

5. Conclusion

In this work, the effect of adding MgO and Al_2O_3 NPs to Rh6G dye solution was investigated through the use of absorption and fluorescence spectra. The main results can be summarized as follows:

1- Addition of NPs enhanced he absorption spectrum of Rh6G, particularly in the case of Al_2O_3 NPs.

2- Addition of NPs quenched the quench the fluorescence spectrum of Rh6G.

3- There exists a strong relationship between donors and acceptors, particularly in the case of Al_2O_3 NPs where the R^2 factor is almost 1.

4- The efficiency of energy transfer in MgO NPs is better than in Al_2O_3 NPs for the studied Rh6G solutions.

ACKNOWLEDGEMENTS

The authors would like to thank Department of Physics, College of Science, Mustansiriyah University (www.uomustansiriyah.edu.iq) Baghdad-Iraq for its support in the present work.

Reference

A.Barik,S.Nath, H. P. (2003) 'Effect of solvent polarity on the photophysical properties of coumarin dye', Chinese Journal of Physics, 119, pp. 10202–10208.

Abdullah, M. M. (2021) 'Dielectric spectroscopy of aluminum oxide (γ-Al2O3)', Kuwait Journal of Science, 49(**2**), pp. 1–12.

Al-Kadhemy, M. F. H., Abbas, K. N. and Abdalmuhdi, W. B. (2020) 'Physical Properties of Rhodamine 6G Laser Dye Combined in Polyvinyl Alcohol films as Heat Sensor', IOP Conference Series: Materials Science and Engineering, 928(**7**), pp. 1–10.

Al-Kadhemy, M. F. H., Hussein, R. and Ali A. Dawood Al-Zuky (2012) 'Analysis of the Absorption Spectra of Styrene-butadiene in Toluene', Journal of Physical Science, 23(1), pp. 89–100.

Ali, A. A. and Zainab F. Mahdi (2012) 'Investigation of nonlinear optical properties for laser dyes-doped polymer thin film', Iraqi Journal of Physics, 10(**19**), pp. 54–69.

Ali, R. *et al.* (2020) 'Green synthesis and the study of some physical properties of MgO nanoparticles and their antibacterial activity', Iraqi Journal of Science, 61(**2**), pp. 266–276.

Błaszkiewicz, P., Kotkowiak, M. and Dudkowiak, A. (2017) 'Fluorescence quenching and energy transfer in a system of hybrid laser dye and functionalized gold nanoparticles', Journal of Luminescence, 183, pp. 303–310.

Chavali, M. S. and Nikolova, M. P. (2019) 'Metal oxide nanoparticles and their applications in nanotechnology', SN Applied Sciences, 1(**6**), pp. 1–30.

Chen, Z. *et al.* (2008) 'Fluorescence spectral properties of rhodamine 6G at the silica/water interface', Journal of Fluorescence, 18(**1**), pp. 93–100.

Kareem, F. F., Saeed, A. A. and Kadhemy, M. F. H. A.- (2021) 'Inspect the Influence of Solvents , Magnesia and Alumina Nanoparticles on Rhodamine 6G Laser Dye Spectroscopic Properties', Journal of Global Scientific Research, 6(**9**), pp. 1695–1709.

Kruszewski, S. and Cyrankiewicz, M. (2013) 'Rhodamine 6G as a mediator of silver nanoparticles aggregation', Acta Physica Polonica A, 123(**6**), pp. 965–969.

Lewkowics and Lakowicz, J. R. (2006) principles of fluorescence spectroscopy. third edit, Principles of Fluorescence Spectroscopy. third edit. springer.

Lide, D. R. (2010) CRC handbook of chemistry and physics. 90 Ed. Taylor and Francis Group LLC.

Lin, C., Katla, S. K. and Perez-Mercader, J. (2021) 'Enhanced fluorescence emission from rhodamine 6G dye through polymerization-induced self-assembly', Journal of Photochemistry and Photobiology A: Chemistry, 406(September 2020), p. 112992.

Mokashi, V. V., Patil, S. R. and G.B.Kolekar (2012) 'Evaluation of interparticle interaction between colloidal Ag nanoparticles coated with trisodium citrate and safranine by using FRET: Spectroscopic and mechanistic approach', J. Photoch. Photobiol. B, 113, pp. 63–69.

Moorthy, S. K. *et al.* (2015) 'MgO Nanoparticles Neem Leves through Green Method', Materials Today: Proceedings, 2(**9**), pp. 4360–4368.

Saeed, A. A., Al-Kadhemy, M. F. H. and Al-Arab, H. S. (2018) 'Energy Transfer Efficiency of Silver Nanoparticles with Rhodamine 6G Dye', Journal College of Education, 1, pp. 1–8.

Stojanovic, B., Bukvic, M. and Epler, I. (2018) 'Application of aluminum and aluminum alloys in engineering', Applied Engineering Letters, 3(2), pp. 52–62.

Terdale, S. and Tantray, A. (2017) 'Spectroscopic study of the dimerization of rhodamine 6G in water and different organic solvents', Journal of Molecular Liquids, 225, pp. 662–671.

Thompson, M. J. and Messina, M. (2019) 'A Quantitative Explanation of the Dynamics Underlying the Franck-Condon Principle: A Mostly Classical Viewpoint', Materials Today: Proceedings. First Edit, 5(**2**), pp. 1–10.

Wahba, M. E. K., El-Enany, N. and Belal, F. (2015) 'Application of the Stern-Volmer equation for studying the spectrofluorimetric quenching reaction of eosin with clindamycin hydrochloride in its pure form and pharmaceutical preparations', Analytical Methods, 7(**24**), pp. 10445–10451.

Yang, M., Xi, X. and Yang, P. (2005) 'The equal-efficiency-proving of fluorescence quenching and enhancement equation', Chinese Science Bulletin, 50(**22**), pp. 2571–2574.

Yun, C. S., Javier, A. and Strouse, G. F. (2005) 'Nanometal Surface Energy Transfer in Optical Rulers, Breaking the FRET Barrier', American Chemical Society, 127, pp. 3115–3119.

Zhang, J., Wang, P. C. and Liang, X. J. (2015) 'In vivo tumortargeted dual-modal fluorescence/CT imaging using a nanoprobe co-loaded with an aggregation-induced emission dye and gold nanoparticles', Biomaterials, 42, pp. 103–111.

Submitted: 20/12/2021
Revised: 23/05/2022
Accepted: 05/06/2022
DOI: 10.48129/kjs.17831